

Time-Dependent Density-Functional Theory for the Stopping Power of an Interacting Electron Gas for Slow Ions

V. U. Nazarov,^{1,2} J. M. Pitarke,^{3,4} C. S. Kim,¹ and Y. Takada²

¹*Department of Physics and Institute for Condensed Matter Theory,
Chonnam National University, Gwangju 500-757, Korea*

²*Institute for Solid State Physics, University of Tokyo, Kashiwa, Chiba 277-8581, Japan*

³*Materia Kondentsatuaren Fisika Saila, Zientzi Fakultatea, Euskal Herriko Unibertsitatea,
644 Posta Kutxatila, E-48080 Bilbo, Basque Country, Spain*

⁴*Donostia International Physics Center and Centro Mixto CSIC-UPV/EHU, Donostia, Basque Country, Spain*

(Dated: August 15, 2018)

Based on the time-dependent density-functional theory, we have derived a rigorous formula for the stopping power of an *interacting* electron gas for ions in the limit of low projectile velocities. If dynamical correlation between electrons is not taken into account, this formula recovers the corresponding stopping power of *noninteracting* electrons in an effective Kohn-Sham potential. The correlation effect, specifically the excitonic one in electron-hole pair excitations, however, is found to considerably enhance the stopping power for intermediately charged ions, bringing our theory into good agreement with experiment.

PACS numbers: 71.10.Ca, 71.15.Mb, 78.70.-g, 78.90.+t

The concept of electron correlation permeates many subfields of condensed matter physics, but it is rather difficult to find good examples of its clear manifestation. It is even more difficult to unambiguously display its importance in time-dependent processes. Here we report a success in obtaining a clean theoretical formula directly relating dynamical correlation, as characterized by the exchange-correlation (xc) kernel of time-dependent density-functional theory (TDDFT), with the experimentally observed stopping power (SP) of solids for slow ions.

The nonperturbative theory of scattering of *noninteracting* electrons by a central potential combined with the density-functional theory (DFT) of Hohenberg, Kohn, and Sham^{1,2} has proved successful in calculating the SP of an electron gas (EG) for slow ions.³ This scheme accurately reproduces the measured energy loss of slow protons and antiprotons in a variety of solids and successfully accounts for the observed oscillatory behavior in the energy loss of slow ions with increasing charge, which is known to originate from the formation of closed shells of bound states around the ion.⁴ These calculations were extended to projectile velocities approaching the Fermi velocity of the target,⁵ but few attempts have been made to include the effect of many-body dynamical correlation that is absent in the current DFT schemes.⁶

In this Communication, we address the effect of dynamical correlation and we employ TDDFT⁷ to derive a rigorous formula for the friction coefficient (SP divided by the projectile velocity at its zero value) of an *interacting* EG. This formula fully includes the effect of dynamical correlation through the imaginary part of a frequency-dependent xc kernel, and it reduces in the absence of dynamical correlation to the SP of noninteracting Kohn-Sham (KS) electrons first reported by Echenique *et al.*³

By adoption of the widely used local-density approximation (LDA), our formula allows us to make a reasonably accurate evaluation of the friction coefficient of

an interacting EG as a function of the projectile charge Z_1e for Z_1 less than about 15. Our calculations indicate that dynamical correlation considerably enhances the SP of slow ions, which is due to the excitonic effect in the electron-hole (e-h) pair excitations. In particular, this effect makes the ratio of maximum to minimum values in the Z_1 -oscillatory behavior of the SP to decrease, leading to better agreement with experiment.

We consider a recoilless probe particle of charge Z_1e moving with velocity \mathbf{v} in an otherwise homogeneous gas of interacting electrons at zero temperature. The average energy lost per unit length traveled by the probe particle (the so-called stopping power of the target) is simply the retarding force that the polarization charge distribution in the vicinity of the projectile exerts on the projectile itself. Accordingly, one can write (we use atomic units)⁸

$$-\frac{dE}{dx} = \frac{Z_1}{v} \int d\mathbf{r} d\mathbf{r}' \delta(\mathbf{r}-\mathbf{v}t) \mathbf{v} \cdot \nabla_{\mathbf{r}} n^{ind}(\mathbf{r}', t) / |\mathbf{r}-\mathbf{r}'|, \quad (1)$$

n^{ind} being the electron density induced by the projectile.

Our starting point is the following rigorous expression for the friction coefficient of an *interacting* electron gas:

$$Q = \frac{1}{8\pi^3} \int d\mathbf{q} d\mathbf{k} v_{\mathbf{q}} v_{\mathbf{k}} \frac{(\mathbf{q} \cdot \mathbf{v})(\mathbf{k} \cdot \mathbf{v})}{v} \frac{\partial}{\partial \omega} \text{Im} \chi_{\mathbf{q}, \mathbf{k}}(\omega) \Big|_{\omega=0}, \quad (2)$$

where $v_{\mathbf{q}} = -4\pi Z_1/q^2$ is the Fourier transform of the bare Coulomb interaction and $\chi_{\mathbf{q}, \mathbf{k}}(\omega)$ is the double Fourier transform of the linear density-response function of a system of *interacting* electrons in the static field of an impurity of charge Z_1 at $\mathbf{r} = 0$. In order to prove Eq. (2), we first expand the right-hand side of Eq. (1) in powers of Z_1 and we then exploit the symmetry properties of many-fold density-response functions to demonstrate that this expansion divided by the projectile velocity at its zero value exactly coincides (to all orders in Z_1) with

the corresponding expansion of the friction coefficient of Eq. (2).⁹

The density-response function $\chi_{\mathbf{q},\mathbf{k}}(\omega)$ depends on the *unknown* ground and excited states of a many-electron system and is, therefore, difficult to calculate. Nevertheless, TDDFT allows us to express $\chi_{\mathbf{q},\mathbf{k}}(\omega)$ as a solution of the integral equation¹⁰

$$\chi_{\mathbf{q},\mathbf{k}}(\omega) = \int d\mathbf{p} \tilde{\epsilon}_{\mathbf{q},\mathbf{p}}^{-1}(\omega) \chi_{\mathbf{p},\mathbf{k}}^0(\omega), \quad (3)$$

where $\tilde{\epsilon}_{\mathbf{q},\mathbf{k}}^{-1}(\omega)$ represents the so-called inverse test-charge-electron dielectric function,

$$\tilde{\epsilon}_{\mathbf{q},\mathbf{k}}^{-1}(\omega) = \delta_{\mathbf{q},\mathbf{k}} - \int d\mathbf{p} \chi_{\mathbf{q},\mathbf{p}}(\omega) [(4\pi/p^2) \delta_{\mathbf{p},\mathbf{k}} + f_{\mathbf{p},\mathbf{k}}^{xc}(\omega)], \quad (4)$$

and $f_{\mathbf{q},\mathbf{k}}^{xc}(\omega)$ is the Fourier transform of the xc kernel

$$f^{xc}[n_0](\mathbf{r}, \mathbf{r}'; \omega) = \delta v^{xc}[n](\mathbf{r}, \omega) / \delta n(\mathbf{r}', \omega)|_{n=n_0}, \quad (5)$$

with $v_{xc}[n](\mathbf{r}, \omega)$ being the frequency-dependent xc potential. $\chi_{\mathbf{q},\mathbf{k}}^0(\omega)$ is the Fourier transform of the density-response function of *noninteracting* KS electrons, i.e., independent electrons in the effective KS potential

$$\tilde{v}(\mathbf{r}) = -Z_1/r + \int d\mathbf{r}' n_0(\mathbf{r}')/|\mathbf{r} - \mathbf{r}'| + v^{xc}[n_0](\mathbf{r}), \quad (6)$$

with $v^{xc}[n_0](\mathbf{r})$ being the static xc potential at the electron density $n_0(\mathbf{r})$. The unperturbed density $n_0(\mathbf{r})$ is obtained by solving self-consistently the KS equations of DFT with the effective potential $\tilde{v}(\mathbf{r})$ of Eq. (6). At $\omega = 0$, we find the following sum rules:

$$\int d\mathbf{q} d\mathbf{k} \begin{pmatrix} \tilde{v}_{\mathbf{q}} \chi_{\mathbf{q},\mathbf{k}}^0(0) \\ v_{\mathbf{q}} \chi_{\mathbf{q},\mathbf{k}}(0) \\ v_{\mathbf{q}} \tilde{\epsilon}_{\mathbf{q},\mathbf{k}}^{-1}(0) \end{pmatrix} = \mathbf{k} \begin{pmatrix} -n_{\mathbf{k}}^0 \\ -n_{\mathbf{k}}^0 \\ \tilde{v}_{\mathbf{k}} \end{pmatrix}, \quad (7)$$

where $n_{\mathbf{q}}^0$ and $\tilde{v}_{\mathbf{q}}$ are the Fourier transforms of the density $n_0(\mathbf{r})$ and the potential $\tilde{v}(\mathbf{r})$. With the aid of these sum rules, substitution of Eq. (3) into Eq. (2) yields

$$Q = Q_1 + Q_2, \quad (8)$$

where

$$Q_1 = \frac{1}{8\pi^3} \int d\mathbf{q} d\mathbf{k} \tilde{v}_{\mathbf{q}} \tilde{v}_{\mathbf{k}} \frac{(\mathbf{q} \cdot \mathbf{v})(\mathbf{k} \cdot \mathbf{v})}{v} \frac{\partial \text{Im} \chi_{\mathbf{q},\mathbf{k}}^0(\omega)}{\partial \omega} \Big|_{\omega=0}, \quad (9)$$

$$Q_2 = -\frac{1}{8\pi^3} \int d\mathbf{q} d\mathbf{k} n_{\mathbf{q}}^0 n_{\mathbf{k}}^0 \frac{(\mathbf{q} \cdot \mathbf{v})(\mathbf{k} \cdot \mathbf{v})}{v} \frac{\partial \text{Im} f_{\mathbf{q},\mathbf{k}}^{xc}(\omega)}{\partial \omega} \Big|_{\omega=0}. \quad (10)$$

Equations (8)-(10), which describe the SP of an interacting many-electron system in the low-velocity limit, show that the low-velocity SP of *interacting* electrons [Eq. (2)] can be obtained as the sum of (i) the SP of *noninteracting* KS electrons [Eq. (9)] and (ii) an excitonic contribution [Eq. (10)], which accounts for the *dynamical* correlation that is absent in Eq. (9).

In order to show that the SP of Eq. (9) is precisely the SP reported in Ref. 3 under the assumption of individual elastic electron scattering by the effective KS potential of Eq. (6), we write an explicit expression for the imaginary part of $\chi_{\mathbf{q},\mathbf{k}}^0(\omega)$ by using incoming and outgoing single-particle states, $|\mathbf{p}'^{(-)}\rangle$ and $|\mathbf{p}^{(+)}\rangle$, and the corresponding single-particle energies, $\varepsilon_{\mathbf{p}'}$ and $\varepsilon_{\mathbf{p}}$.²³

$$\text{Im} \chi_{\mathbf{q},\mathbf{k}}^0(\omega) = (2\pi)^{-2} \int d\mathbf{p} d\mathbf{p}' [f(\varepsilon_{\mathbf{p}'}) - f(\varepsilon_{\mathbf{p}})] \delta(\omega - \varepsilon_{\mathbf{p}} + \varepsilon_{\mathbf{p}'}) \times \langle \mathbf{p}'^{(-)} | e^{i\mathbf{q}\mathbf{r}} | \mathbf{p}^{(+)} \rangle \langle \mathbf{p}^{(+)} | e^{-i\mathbf{k}\mathbf{r}} | \mathbf{p}'^{(-)} \rangle, \quad (11)$$

where $f(\varepsilon)$ denotes the Fermi distribution function. Substituting Eq. (11) into Eq. (9) and referring to the Lippman-Schwinger equation of scattering theory, one finds

$$Q_1 = \bar{n} k_F \sigma_{tr}(k_F), \quad (12)$$

where k_F is the Fermi momentum, $\sigma_{tr}(q)$ is the so-called transport cross section, and \bar{n} is the density of the homogeneous EG in the absence of the projectile.

An evaluation of Eq. (9) [or, equivalently, Eq. (12)] and Eq. (10) involves the *unknown* quantities $v^{xc}[n_0](\mathbf{r})$ and $f^{xc}[n_0](\mathbf{r}, \mathbf{r}'; \omega)$, respectively. Existing DFT calculations from Eq. (12) have been implemented by invoking the LDA, i.e., by replacing the xc potential $v^{xc}[n_0](\mathbf{r})$ by the xc potential of a homogeneous EG with the local density $n_0(\mathbf{r})$. At the same level of approximation, we use the LDA to evaluate the excitonic contribution of Eq. (10). In this approach, the frequency-dependent (nonadiabatic) xc kernel $f^{xc}[n_0](\mathbf{r}, \mathbf{r}'; \omega)$ is obtained as¹⁷

$$f^{xc}[n_0](\mathbf{r}, \mathbf{r}'; \omega) = f_h^{xc}[n_0(\mathbf{r}), \omega] \delta(\mathbf{r} - \mathbf{r}'), \quad (13)$$

where $f_h^{xc}(n, \omega)$ denotes the $q \rightarrow 0$ limit of the frequency-dependent xc kernel of a homogeneous EG of density n . Due to the spherical symmetry of $n_0(\mathbf{r})$, substitution of Eq. (13) into Eq. (10) yields

$$Q_2 = -\frac{4\pi}{3} \int_0^\infty dr [r n_0'(r)]^2 \frac{\partial \text{Im} f_h^{xc}[n_0(r), \omega]}{\partial \omega} \Big|_{\omega=0}. \quad (14)$$

An explicit expression for the imaginary part of $f_h^{xc}(n, \omega)$ has been reported recently, which is exact at low frequencies to leading order in the Coulomb interaction.¹⁸ Since the frequency derivative entering Eq. (14) is negative definite,¹⁸ this equation shows that dynamical correlation enhances the SP of a system of interacting electrons. This enhancement can be ascribed to the attractive e-h multiple scattering or excitonic effect in the e-h pair excitation.¹⁹

The calculations presented below have been carried out from Eqs. (12) and (14), with use of the LDA xc potential $v^{xc}[n_0](\mathbf{r})$ of Perdew and Zunger²⁰ and the frequency-dependent LDA xc kernel $f_h^{xc}(n, \omega)$ of Qian and Vignale.¹⁸ We have performed calculations for various values of Z_1 and the electron-density parameter $r_s = (3/4\pi\bar{n})^{1/3}$. We have found that dynamical correlation can be neglected at small projectile charges and

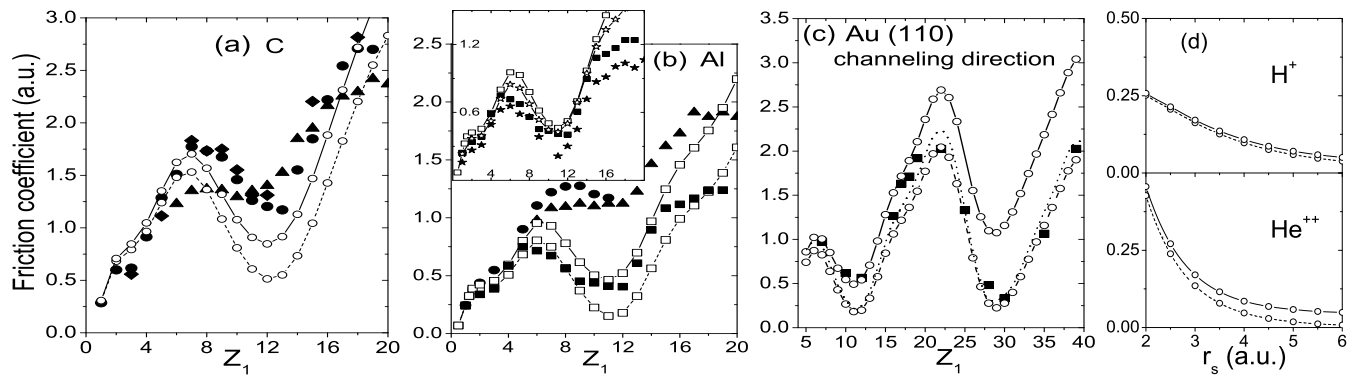


FIG. 1: Friction coefficient of a homogeneous EG versus the projectile charge Z_1 (a)-(c) and the EG-density parameter r_s (d), as obtained in the LDA from Eq. (12) (dashed chained curves) and from the sum of Eqs. (12) and (14) (solid chained curves). (a) Solid circles, triangles, and diamonds are transmission measurements from Refs. 11, 12, and 13 of the random SP of C for ions moving with velocities $v = 0.41, 0.83$, and 0.25 a.u., respectively. (b) Solid circles and triangles are transmission measurements from Refs. 11 and 12 of the random SP of Al for projectiles moving with velocities $v = 0.41$ and 0.83 a.u., respectively. Solid squares (stars in the inset) are the measured SP of Al of Ref. 14 (15) for slow ions ($v = 0.5$ a.u.) moving at a distance of 1.0 (1.2) a.u. from the last atomic row at the surface. (c) Solid squares are the measurements of Ref. 16 of the SP of Au for slow ions ($v = 0.68$ a.u.) channeled along the (110) direction. These measurements are compared to EG calculations with $r_s = 2$. The dotted line is the calculation of Ref. 6 with dynamical xc effects included in the framework of linear-response theory.

high electron densities, where many-body effects play a minor role. At metallic densities ($1.5 < r_s < 6$), however, the correlation effect is found to considerably enhance the SP for intermediately charged ions.

At low velocities, the energy loss of ions in solid materials is mainly due to the stopping power of valence electrons. Since these electrons are known to be well described by a homogeneous EG,²¹ we apply our theory to the cases of C, Al, and Au, and compare the result of our EG calculations to the available experimental data for these materials (see Fig. 1).

First, we compare the results we have obtained for the friction coefficient of a homogeneous EG with $r_s = 1.59$ and $r_s = 2.07$ [solid chained curves in Figs. 1(a) and 1(b)] to the transmission measurements of the random SP for slow ions in C and Al (solid circles, squares and diamonds). If we neglect dynamical correlation (dashed chained curves), our calculations reproduce those of Ref. 4. The effect of dynamical correlation is found to be negligible at low ions charges; however, as Z_1 increases this effect becomes comparable to the SP of noninteracting KS electrons. We observe that the impact of dynamical correlation becomes relatively larger at the formation of closed shells of bound states around the probe particle, where the SP has a local minimum. As a result, the ratio of the maximum to minimum values in the oscillations of the SP decreases in the presence of dynamical correlation, leading to better agreement with experiment.

Differences between our calculation and the transmission measurements of the random SP of C and Al should be partially due to the contribution from elastic collisions of the projectile with the atomic cores of the target, which is not included in our calculation. Hence, we have also considered the measured SP of Al for slow ions moving at a distance of $d = 1.0$ a.u. from the last atomic

row at the surface¹⁴ [solid squares in Fig. 1(b)], which is free from elastic collisions with target atoms. At this distance, the electron density is close to the bulk value ($r_s = 2.07$) and the SP is expected to be only slightly smaller than that for ions moving in a uniform EG.²² Figure 1(b) shows that this is indeed the case, although our many-body calculation (solid chained curve) is too high for $Z_1 > 15$. As Z_1 increases the electron-density variation near the projectile becomes large, and differences between our calculations and the experimental data may, therefore, be ascribed to the failure of the LDA.

To elucidate the effect of the inhomogeneity of the EG near the Al surface, in the inset of Fig. 1(b) we plot again our many-body calculation at $r_s = 2.07$ and the measured data at $d = 1.0$ a.u., but now together with the measured SP of Al for slow ions moving at $d = 1.2$ a.u.¹⁵ (solid stars) and the calculated curve for the corresponding density of $r_s = 2.2$ (solid chained curve with stars). Since the two theoretical curves essentially coincide, this figure shows that at 1.2 a.u., where the gradient of the electron density is considerably larger than that at $d = 1.0$ a.u.,¹⁵ SP is worsly described by the homogeneous EG.

Contributions from elastic collisions with the target atoms should also be absent in channeling experiments, in which the projectile penetrates a solid along a high-symmetry direction. In Fig. 1(c) we compare the experimental data of Ref. 16 (solid squares) for slow ions channeled along the (110) direction in Au with the result of our many-body calculation for the friction coefficient of a homogeneous EG with $r_s = 2.0$. This figure shows that many-body correlation effects tend to decrease the ratio of the maximum to minimum values in the oscillatory behavior of the SP, thus bringing the SP into nice agreement with experiment for projectile charges up to $Z_1 = 19$. However, comparison between theory and ex-

periment at $Z_1 > 19$ suggests that at these large values of Z_1 the strong inhomogeneity of the EG suppresses dynamical correlations and calls for going beyond the LDA.

Finally, Fig. 1(d) displays the interacting and non-interacting SP for H^+ and He^{++} , as a function of r_s . Figure 1(d) shows that (i) the effect of dynamical correlation is very small in the case of H^+ , in which case the electron density variation is comparatively small, and (ii) the dynamical correlation effect becomes comparatively more important as the electron density decreases.

In conclusion, we have presented a rigorous TDDFT for the stopping power of an *interacting* EG in the limit of low projectile velocities. In the absence of dynamical correlation, our theory yields the SP of *noninteracting* KS electrons, which we have shown to be equivalent

to the existing DFT-based elastic electron scattering approach. We have investigated the effect of many-body dynamical correlation by using an accurate representation of the long-wavelength frequency-dependent xc kernel. Our results show that dynamical correlations considerably enhance the SP of intermediately charged ions, thereby bringing the theory into better agreement with the experimentally observed oscillations of the SP for projectiles of charge $Z_1 < 15$. However, at higher values of Z_1 , one needs to go beyond the LDA in the description of the dynamical xc effects.

V.U.N. and C.S.K. acknowledge support by the Korea Research Foundation through Grant No. KRF-2003-015-C00214. J.M.P. acknowledges partial support by the UPV/EHU and the MCyT.

-
- ¹ P. Hohenberg and W. Kohn, Phys. Rev. **136**, B864 (1964).
 - ² W. Kohn and L. J. Sham, Phys. Rev. **140**, A1133 (1965).
 - ³ P. M. Echenique, R. M. Nieminen, and R. H. Ritchie, Solid State Commun. **37**, 779 (1981).
 - ⁴ P. M. Echenique, R. M. Nieminen, J. C. Ashley, and R. H. Ritchie, Phys. Rev. A **33**, 897 (1986).
 - ⁵ A. Salin, A. Arnau, P. M. Echenique, and E. Zaremba, Phys. Rev. B **59**, 2537 (1999).
 - ⁶ I. Nagy, A. Arnau, and P. M. Echenique, Phys. Rev. A **40**, 987 (1989).
 - ⁷ E. Runge and E. K. U. Gross, Phys. Rev. Lett. **52**, 997 (1984).
 - ⁸ P. M. Echenique, F. Flores, and R. H. Ritchie, Solid State Phys. **43**, 229 (1990).
 - ⁹ V. U. Nazarov, (unpublished).
 - ¹⁰ M. Petersilka, U. J. Gossmann, and E. K. U. Gross, Phys. Rev. Lett. **76**, 1212 (1996).
 - ¹¹ J. H. Ormrod and H. E. Duckworth, Can. J. Phys. **41**, 1424 (1963), J. H. Ormrod, J. R. Macdonald, and H. E. Duckworth, *ibid.* **43**, 275 (1965).
 - ¹² D. Ward et al., Can. J. Phys. **57**, 645 (1979).
 - ¹³ G. Högborg, Phys. Status Solidi B **46**, 829 (1971).
 - ¹⁴ H. Winter et al., Europhys. Lett. **41**, 437 (1998).
 - ¹⁵ H. Winter et al., Phys. Rev. B **67**, 245401 (2003).
 - ¹⁶ J. Böttiger and F. Bason, Radiat. Effects **2**, 105 (1969).
 - ¹⁷ E. K. U. Gross and W. Kohn, Phys. Rev. Lett. **55**, 2850 (1985).
 - ¹⁸ Z. Qian and G. Vignale, Phys. Rev. B **65**, 235121 (2002).
 - ¹⁹ Y. Takada and H. Yasuhara, Phys. Rev. Lett. **89**, 216402 (2002).
 - ²⁰ J. P. Perdew and A. Zunger, Phys. Rev. B **23**, 5048 (1981).
 - ²¹ I. Campillo, J. M. Pitarke, and A. G. Eguiluz, Phys. Rev. B **58**, 10307 (1998).
 - ²² A. Garcia-Lekue and J. M. Pitarke, Phys. Rev. B **64**, 35423 (2001).
 - ²³ Typically, the same set of eigenfunctions is used for both bra and ket vectors entering Eq. (11). Nevertheless, it can be shown that two different orthonormal complete sets can be used, which we here choose to be the incoming and outgoing states. Although we work with the density-response function of an inhomogeneous EG rather than the force-force correlation function, our proof has much in common with a derivation in: E. G. d'Agliano, P. Kumar, W. Schaich, and H. Suhl, Phys. Rev. B **11**, 2122 (1975).